ASEG-PESA 2015
Geophysics and Geology together for Discovery
24th International Geophysical Conference and Exhibition
15–18 February 2015 Perth, Western Australia

Solving the 3D Acoustic Wave-Equation on Generalized Structured Meshes: A FDTD Approach

Jeffrey Shragge
The University of Western Australia
M004, 35 Stirling Highway
Crawley, WA 6009, Australia
Jeffrey.Shragge@uwa.edu.au

SUMMARY

The key computational kernels of most advanced 3D exploration seismic imaging and inversion algorithms involve calculating solutions of the 3D acoustic wave equation, most commonly with a finite-difference time-domain (FDTD) methodology. While well suited for regularly sampled rectilinear computational domains, FDTD methods seemingly have limited applicability in scenarios involving irregular 3D domain boundaries and mesh interiors best described by non-Cartesian geometry (e.g., surface topography). Using coordinate mappings and differential geometry, I specify a FDTD approach for generating numerical solutions to the acoustic wave equation that is applicable to generalized 3D coordinate systems and (hexahedral) structured meshes. I validate the method on different computational meshes and demonstrate the viability of the modelling approach for 3D non-Cartesian imaging and inversion scenarios.

Key words: Finite difference, reverse-time migration, 3D acoustic wave propagation, seismic modelling.

INTRODUCTION

Calculating numerical solutions of the 3D acoustic wave equation represents the key computational kernel of most advanced 3D seismic imaging and inversion methods currently used in seismic exploration. These algorithms include the high-end 3D seismic techniques of reverse-time migration (RTM), full-waveform inversion (FWI) and wave-equation migration velocity analysis (WEMVA). Finite-difference time-domain (FDTD) methods represent the most common numerical approach for generation solutions of the 3D acoustic wave equation, and have long been developed and increasingly widely implemented since the 1980s (Robertsson *et al.*, 2012). While 3D FDTD modelling of acoustic wavefields is fairly straightforward for regularly sampled rectilinear meshes, these approaches have seemingly lower applicability for scenarios where seismic data are acquired on surfaces exhibiting irregular topology. Undertaking full-wavefield imaging and velocity inversion experiments in these situations requires handling irregular computational domains that are arguably best described by a more general non-Cartesian geometry. These types of scenarios may be found at many scale lengths, ranging from laboratory imaging experiments using ultrasonic measurements on cylindrical core plugs to seismic exploration scale over free-surface topography or irregular water-bottom surfaces.

One strategy for handling scenarios exhibiting irregular geometry is to turn to integral-based methods that solve the 3D acoustic wave equation on voxelised elements designed to conform to undulating domain boundary surfaces and to infill computational mesh interiors. Examples of these types of approaches include the finite-element (Marfurt, 1984), spectral-element (Komatitsch and Vilotte, 1998) and discontinuous-Galerkin (Cockburn *et al.* 2000) methods. By using meshes conformal to irregular surfaces, these approaches facilitate the numerical implementation of free-surface boundary conditions (Priolo *et al.*, 1994) and are able to more accurately represent discontinuities across major interior lithological boundaries relative to finite-difference methods (Fornberg, 1988).

While the integral-based methods provide highly accurate - though computationally expensive - solutions to the 3D acoustic wave equation, herein I argue that automatically precluding FDTD strategies for scenarios exhibiting irregular geometry and generalized (quadrilaterally faced hexahedral) structured meshes represents a severe and potentially unnecessary restriction. Rather, applying a FDTD methodology on irregular structured meshes is technically feasible and, in many cases, represents a cost-effective computational strategy. A successful implementation, though, requires addressing three key challenges: (1) how to generate a 3D computational domain that conforms to the desired geometry and exhibits favourable mesh characteristics; (2) how to specify the 3D acoustic wave equation appropriate for the irregular computational domain; and (3) how to provide a stable and numerically accurate solution of the 3D acoustic wave equation on that generalized 3D mesh.

Solving partial differential equations on irregularly shaped computational domains using coordinate transformation approaches and finite-difference operators is a common technique for boundary value problems in many science and engineering fields. While these techniques have found a moderate amount of traction for modelling wavefield solutions of 2D/3D (visco)elastic wave equations (Ohminato *et al.*, 1997; Hestholm, 1999; Appelo and Petersson, 2009), they are seldom used to solve the two-way acoustic wave equation for 3D full-wavefield imaging and velocity inversion problems.

The acoustic propagation methodology advocated herein represents an adaptation of the Riemannian wavefield extrapolation (RWE) coordinate transform approach that uses differential geometry relationships and known mappings between 3D generalized and Cartesian coordinate systems to specify the Laplacian differential operator governing 3D acoustic wave propagation in that generalized coordinate system. Sava and Fomel (2005) present a derivation of RWE for acoustic wave propagation in 2D semi-orthogonal ``Riemannian coordinates'' and implement a one-way operator appropriate for 2D wave-equation migration (WEM). Shragge (2008) extends this approach to 3D non-orthogonal coordinates and similarly implements a one-way operator for 3D WEM imaging. Shragge (2014) demonstrates the applicability of this method for two-way acoustic wave equations and applies the developed FDTD operators to perform 2D RTM directly from topographic surfaces. Building on from these approaches, the goals of the present work are three-fold: (1) to provide an extension of RWE theory to the two-wave acoustic wave equation for generalized (non-orthogonal) 3D geometries; (2) to demonstrate that one can develop generalized-coordinate $O(\Delta t^2,\Delta x^8)$ FDTD operators that are (nearly) equivalent to standard Cartesian $O(\Delta t^2,\Delta x^8)$ FDTD operators; and (3) to highlight some of the potential uses of the method for 3D acoustic wave propagation problems exhibiting non-Cartesian geometry.

I begin by presenting the theory of the 3D (constant-density) acoustic wave equation in generalized 3D coordinate systems based on coordinate mapping and differential geometry relationships. I then detail a numerical FDTD solution of the 3D acoustic wave equation that takes into account the spatial variability of non-Cartesian geometry. Finally, I test the developed theory and the numerical scheme on two different computational meshes: an ``internal boundary'' mesh conforming to a dipping water bottom, and an ``topographic'' coordinate mesh conforming to an irregular free surface.

GENERALIZED ACOUSTIC WAVE EQUATION

The acoustic wave equation in a 3D generalized coordinate system defined by variables $\boldsymbol{\xi} = [\xi_1,\xi_2,\xi_3]$ is given by

$$\left[\nabla^2_\xi - \frac{1}{v_\xi^2}\frac{\partial^2}{\partial t^2}\right]U_\xi = F_\xi \tag{1}$$

where ∇^2_ξ is a generalized Laplacian operator, v_ξ is a velocity field, U_ξ is a scalar acoustic wavefield, and F_ξ is the source distribution. Herein, I use a notation where subscripts $\boldsymbol{\xi}$ designate fields and operators defined in the generalized $\boldsymbol{\xi}$-coordinate system, while those in Cartesian coordinate system $\mathbf{x}=[x_1,x_2,x_3]$ are specified by a subscript $\mathbf{x}$. Cartesian $\mathbf{x}$-coordinates represent a physical domain over which one desires to calculate a solution to the acoustic wave equation. Generalized $\boldsymbol{\xi}$-coordinates represent a transformed canonical domain on which one actually computes an acoustic wavefield solution. The relationship between the $\boldsymbol{\xi}$- and $\mathbf{x}$-coordinate systems is assumed to be known, unique (i.e., one-to-one), and expressible through a set of analytical or numerical mapping equations, $x_i=f_i(\xi_j)$ where i,j = 1,2,3.

Because the partial differential operators of the generalized Laplacian are specified in the $\boldsymbol{\xi}$-coordinate system, they naturally are affected by spatially varying geometry. Providing the correct formulation of the Laplacian operator on the $\boldsymbol{\xi}$-mesh involves introducing transformations from the mathematical field of differential geometry in the form of the (symmetric rank-two) metric tensor, $[g_{ij}]$, whose elements provide a link between the $\boldsymbol{\xi}$- and $\mathbf{x}$-coordinate systems:

$$g_{ij} = \frac{\partial x_k}{\partial \xi_i}\frac{\partial x_k}{\partial \xi_j}, \tag{2}$$

where summation notation over repeated indices is assumed and subscript and superscript indices on matrices (i.e., g_{ij} and g^{ij}) indicate covariant and contravariant tensors, respectively (Synge and Schild, 1978).

Specifying the acoustic wave equation in generalized coordinates requires using a contravariant representation of the metric tensor defined as the matrix inverse of the covariant metric tensor. Computing the partial derivatives of the Laplacian operator in equation 1 involves introducing the contravariant metric tensor elements into a generalized expression for the Laplacian operator (Guggenheimer, 1977). When substituted into equation 1, one recovers the following generalised 3D acoustic wave equation

$$\zeta_i \frac{\partial U_\xi}{\partial \xi_i} + g^{ij}\frac{\partial^2 U_\xi}{\partial \xi_i \partial \xi_j} = \frac{1}{v_\xi^2}\frac{\partial^2 U_\xi}{\partial t^2} + F_\xi, \tag{3}$$

where, for brevity, I write first-order coefficients ζ^i as

$$\zeta^i = \frac{1}{\sqrt{|g|}}\frac{\partial\left(\sqrt{|g|}g^{ij}\right)}{\partial \xi_j} \tag{4}$$

and $|\mathbf{g}|$ is the metric tensor discriminant.

GENERALIZED FDTD PROPAGATION

Specifying a 3D FDTD propagation scheme appropriate for generating numerical solutions of the 3D acoustic wave equation in generalized structured meshes is a relatively straightforward undertaking that requires only two minor modifications to established Cartesian-coordinate FDTD approaches. First, one must account for the spatially varying metric tensor components when applying FD stencils to discretized wavefields. Second, one needs to incorporate both first- and mixed second-order partial derivatives, as well as the standard second-order partial derivatives, of the generalized Laplacian operator in equation 3.

The proposed FDTD scheme is based on finite-difference approximations of order $O(\Delta x^8)$ for the spatial first- and second-order derivative operators and an $O(\Delta x^4)$ approximation of the mixed second-order partial derivatives (where Δx is the sampling interval in the canonical domain). Continuous wavefields are approximated by a discrete representation, $U_\xi(\xi,t) = U^p_{l,m,n}$, where l=[1,L], m=[1,M] and n=[1,N] are spatial indices and p=[1,P] is the temporal index. Similarly, the continuous and time-independent ζ^i fields and g^{ij} metric tensor components are represented by $\zeta^i_{l,m,n}$ and $g^{ij}_{l,m,n}$. Given these representations and assuming that discretization of the computational mesh is uniform in all directions (i.e., $\Delta\xi=\Delta\xi_1=\Delta\xi_2=\Delta\xi_3$), I rewrite the spatial first-order partial-derivative FD operators as, e.g.,

$$\zeta^1\frac{\partial U_\xi}{\partial \xi_1} \approx \frac{\zeta^1_{l,m,n}}{\Delta\xi}\sum_{i=1}^{4}\Phi_i\left[U^p_{l+i,m,n} - U^p_{l-i,m,n}\right] \tag{5}$$

where similar approximations exist for the other first-order partial derivatives. I write the second-order partial-derivative FD operators as, e.g.,

$$g^{11}\frac{\partial^2 U_\xi}{\partial \xi_1^2} \approx \frac{g^{11}_{l,m,n}}{\Delta\xi}\sum_{i=1}^{4}\Sigma_i\left[U^p_{l+i,m,n} + U^p_{l-i,m,n}\right] \tag{6}$$

where, again, similar expressions exist for the second-order partial derivatives. I approximate the mixed second-order partial-derivative FD operators as, e.g.,

$$g^{12}\frac{\partial^2 U_x}{\partial x_1 \partial x_2} \approx \frac{g^{12}_{l,m,n}}{\Delta x^2}\sum_{i=1}^{4} M_{ij}\left[U^p_{l+i,m+i,n} + U^p_{l-i,m-i,n} - U^p_{l+i,m-i,n} - U^p_{l-i,m+i,n}\right] \quad (7)$$

where similar expressions exist for the two other mixed second-order partial-derivatives. The FD coefficients F_i, S_i and M_{ij} used in the following examples can be found through standard approximation techniques. Finally, I use a standard $O(\Delta t^2)$ approximation for the second-order temporal derivative term that, when combined with expressions like those in equations 5-7 and solving for $U^{p+1}_{l,m,n}$, leads to 3D FDTD propagation scheme for modeling the temporal evolution of an acoustic wavefield on a generalized 3D coordinate mesh.

NUMERICAL EXAMPLES

This section investigates 3D acoustic wave propagation on two different coordinate meshes: ``internal boundary'' (IB) coordinates conforming to an irregular seafloor surface and ``topographic'' coordinates conforming to an irregular free surface. These computational meshes provide informative tests of both the generalized 3D acoustic wave-equation theory and of the implementation of the 3D FDTD numerical scheme described above.

One potential use of generalized 3D coordinate systems is to create meshes that are conformal to irregular internal boundaries, such as those at major lithological interfaces (e.g. seafloor, geologic unconformities, etc; c.f. Figure 1). By aligning the coordinate mesh with these boundaries one can reduce - or potentially eliminate – many of the deleterious discretization artifacts (e.g., stair-casing) commonly observed in Cartesian wavefield simulation through dipping interfaces. Moreover, this approach can also be used to improve algorithmic efficiency, such as allowing for wavefield injection of data from ocean bottom cable (OBC) or node (OBN) datasets along a single interface conformal to irregular sea-floor topography.

Generating meshes conformal to one or more generic parametric surfaces can be accomplished by employing Bézier interpolating functions. Herein, I present an example of a 3D coordinate system conforming to: (1) the free-surface boundary; (2) a uniformly flat layer at depth; and (3) an irregular water-bottom surface. Note that the resulting mapping relationship between the two coordinate systems (c.f. Figure 1) defines the geometric coefficients in equation 3 and thereby the specific generalised 3D acoustic wave equation to be solved. Importantly, in the context of this work, because the 3D internal boundary (IB) coordinate system exactly conforms to a 3D Cartesian mesh at the surface and at a constant depth level, this computational mesh allows for a direct evaluation of the numerical accuracy of the above 3D FDTD scheme relative to the equivalent Cartesian FDTD scheme, and thus represents an important numerical verification of the described approach.

Figure 2 presents the constant velocity 3D impulse response computed in 3D IB coordinates and then interpolated back to a Cartesian mesh. Note that the impulse response is hemispherical as demanded by theory. To better test the accuracy of the numerical scheme I compute the impulse response through a Cartesian mesh using Cartesian FDTD operators of the same order. Figure 3 presents a waveform comparison between the results computed in IB (green) and Cartesian (red) coordinates as well as the waveform difference (black). The waveform fit is very good, though the Cartesian waveform exhibits a very slight delay with respect to the IB waveforms (i.e., by less than a single time sample) and thus does not provide a perfect match. Overall, this example demonstrates the IB meshes can be specified and used in 3D acoustic propagation kernels for RTM and FWI applications.

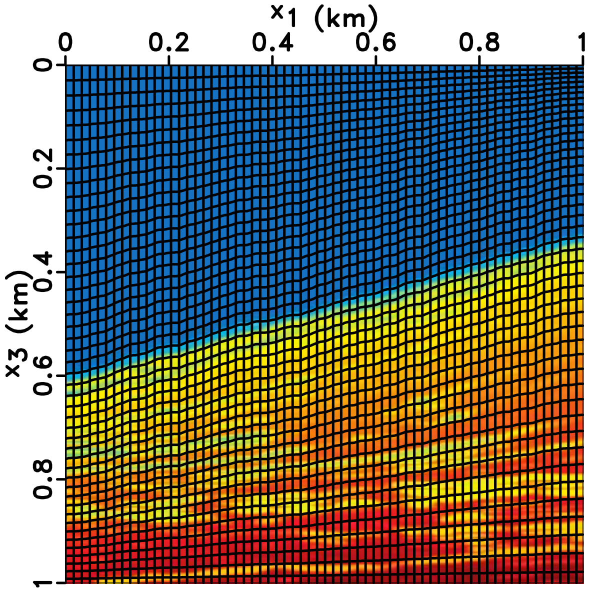

Figure 1. 2D volume slice extracted from 3D IB coordinate system. Note that a single depth contour of mesh has been made to conform to the irregular sea bottom.

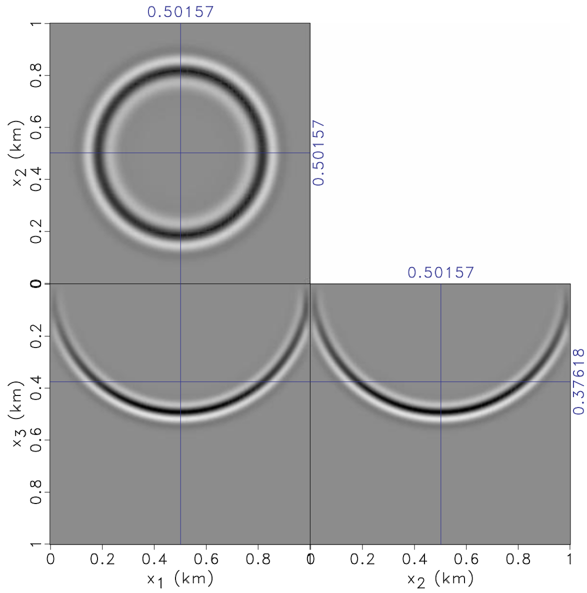

Figure 2. 3D constant velocity impulse response simulated through the 3D IB coordinates mesh and then interpolated back to Cartesian coordinates.

A second application of the proposed 3D FDTD acoustic propagation scheme is simulating wavefields directly from topographic surfaces. This remains a numerical challenge commonly encountered during 3D prestack depth migration and FWI of land seismic data. Similar to above, I use (linear) Bézier interpolating functions to construct a 3D computational mesh that is conformal to both a topographically influenced free surface and a constant depth level. Again, the mapping relationship between the ξ- and $\mathbf{x}$-coordinate systems defines the geometric coefficients and thereby the specific generalised 3D acoustic wave equation to be solved.

Figure 4 presents an example of acoustic wave propagation simulated in topographic coordinates and subsequently interpolated back to the Cartesian mesh. (The topographic free surface is overlain for reference.) This example shows the downward propagating hemispherical wavefront, as well as significant scattering from free-surface topography. Note that because the coordinate mesh conforms to the free surface, it is easy to apply the free-surface boundary condition and replicate full wavefield effects without introducing commonly observed Cartesian staircasing phenomena.

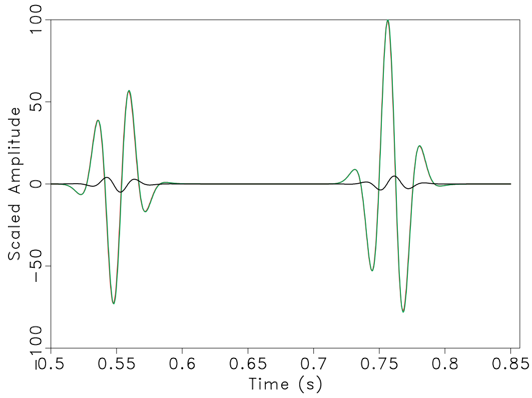

Figure 3. Numerical accuracy test comparing waveforms simulated in IB (green) and Cartesian (red) coordinates along with the waveform difference (black).

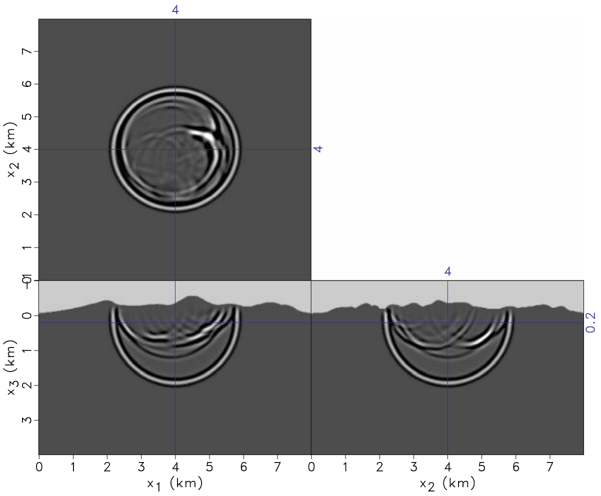

Figure 4. Example of 3D acoustic wave propagation in “Topographic coordinates” (following an interpolation back to a Cartesian mesh for visualisation purposes).

CONCLUSIONS

Applying 3D FDTD acoustic wave propagation on generalized structured meshes is feasible using a combination of coordinate mappings and differential geometry. The two key changes relative to a Cartesian 3D FDTD implementation are introducing first- and mixed second-order derivatives as well as geometric scaling factors to account for the effects of spatially varying geometry when computing 3D acoustic wave-equation solutions. The examples demonstrate that stable and accurate solutions of the 3D acoustic wave equation can be found using a generalized coordinate FDTD strategy. Finally, the generalized 3D FDTD approach provides accurate 3D impulse responses and thus can be used as the computational kernel for non-Cartesian 3D imaging and velocity inversion experiments such as RTM, FWI and WEMVA and, potentially, related 3D FDFD FWI approaches.

ACKNOWLEDGMENTS

I thank the UWA:RM consortium sponsors for providing resources to enable this research. Reproducible examples were completed using the Madagascar package (www.ahay.org).

REFERENCES

Appelo, D., and Petersson, N.A., 2009, A stable finite-difference method for the elastic wave equation on complex geometries with free surfaces: Communications in Computational Physics, 5, 84–107.

Cockburn, B., Karniadakis, G., and Shu, C., 2000, Discontinuous Galerkin methods: Theory, computational and applications: Springer-Verlag.

Fornberg, B., 1988, Generation of finite difference formulas on arbitrarily spaced grids: Mathematics of Computation, 51, 699–706.

Guggenheimer, H., 1977, Differential geometry: Dover Publications, Inc., New York.

Hestholm, S., 1999, Three-dimensional finite difference viscoelastic wave modelling including surface topography: Geophysical Journal International, 139, 852–878.

Komatitsch, D., and Vilotte, J.-P., 1998, The spectral element method: An efficient tool to simulate the response of 2D and 3D geological structures: Bulletin of the Seismological Society of America, 88, 368–392.

Marfurt, K., 1984, Accuracy of finite-difference and finite-element modelling of the scalar and elastic wave equations: Geophysics, 49, 533–549.

Ohminato, T., and Chouet, B.A., 1997, A free-surface boundary condition for including 3D topography in the finite-difference method: Bulletin of the Seismological Society of America, 87, 494–515.

Priolo, E., Carcione, J. and Seriani, G., 1994, Numerical simulation of interface waves by high-order spectral modeling techniques: Journal of the Acoustical Society of America, 95, 681–693.

Robertsson, J., Blanch, J.O., Nihei, K., and Troemp, J. (Editors), 2012, Numerical Modeling of Seismic Wave Propagation: Gridded Two-way Wave-equation Methods: SEG, Geophysics Reprint Series 28.

Sava, P., and Fomel, S., 2005, Riemannian wavefield extrapolation: Geophysics, 70, no. 3, T45–T56.

Shragge, J., 2008, Riemannian wavefield extrapolation: Non-orthogonal coordinate systems: Geophysics, 73, no. 2, T11–T21.

———, 2014, Reverse time migration from topography: Geophysics, 79, no. 4, T1–T12.

Synge, J.L., and Schild, A., 1978, Tensor Calculus: Dover Publications, Inc., New York.